

Ghost propagator and ghost-gluon vertex from Schwinger-Dyson equations

A. C. Aguilar,¹ D. Ibáñez,² and J. Papavassiliou²

¹*University of Campinas - UNICAMP,*

Institute of Physics “Gleb Wataghin”, 13083-859 Campinas, SP, Brazil

²*Department of Theoretical Physics and IFIC, University of Valencia and CSIC,
E-46100, Valencia, Spain*

Abstract

We study an approximate version of the Schwinger-Dyson equation that controls the nonperturbative behavior of the ghost-gluon vertex, in the Landau gauge. In particular, we focus on the form factor that enters in the dynamical equation for the ghost dressing function, in the same gauge, and derive its integral equation, in the “one-loop dressed” approximation. We consider two special kinematic configurations, which simplify the momentum dependence of the unknown quantity; in particular, we study the soft gluon case, and the well-known Taylor limit. When coupled with the Schwinger-Dyson equation of the ghost dressing function, the contribution of this form factor provides considerable support to the relevant integral kernel. As a consequence, the solution of this coupled system of integral equations furnishes a ghost dressing function that reproduces the standard lattice results rather accurately, without the need to artificially increase the value of the gauge coupling.

PACS numbers: 12.38.Aw, 12.38.Lg, 14.70.Dj

I. INTRODUCTION

One of the few nonperturbative frameworks available for the study of the infrared sector of QCD in the continuum are the Schwinger-Dyson equations (SDEs), which govern the dynamics of the basic Green's functions of the theory [1–4]. Despite the well-known limitations intrinsic to this formalism, a variety of theoretical and technical advances have provided new valuable insights on some of the most fundamental nonperturbative phenomena of QCD, such as quark confinement, dynamical mass generation, and chiral symmetry breaking [3, 5–8]. Particularly important in this ongoing effort is the systematic confrontation of the SDE predictions with the results of large-volume lattice simulations [9–14], leading not only to quantitative refinements, but, in some cases, to critical revisions of the underlying physical concepts [7, 15–17].

The quantitative understanding of the ghost sector of QCD constitutes a long-standing challenge for the SDE practitioners. Without a doubt, the most fundamental quantity in this context is the ghost propagator, $D(p^2)$, and the corresponding dressing function, $F(p^2) = p^2 D(p^2)$; in fact, the infrared behavior of the latter, in the Landau gauge (LG), has been traditionally associated with a particular realization of color confinement [18–21].

In recent years, various lattice studies, both in $SU(2)$ and $SU(3)$, together with numerous analytic approaches, find a massless ghost propagator with an infrared finite dressing function [7, 9, 11, 17, 22]. In addition, in the same gauge, the gluon propagator obtained on the lattice is finite in the deep infrared, supporting the notion of an effectively massive gluon. In fact, the dynamical gluon mass generation, first proposed in [23], and further developed in a number of recent works, provides a unified explanation for the observed finiteness of both aforementioned quantities [7, 24–27]. Specifically, an infrared finite $F(p^2)$ emerges as a direct consequence of the massiveness of the gluon propagator: such a gluon propagator, when inserted in the SDE of the ghost propagator, saturates the logarithms associated with the $F(p^2)$, thus making it finite at the origin.

However, what has been more difficult to obtain from a self-consistent SDE analysis is the entire shape and size of $F(p^2)$ provided by the lattice [7, 28]. In fact, even when one substitutes into the ghost SDE the gluon propagator furnished by the lattice, but keeping the ghost-gluon vertex at its tree-level value, the resulting $F(p^2)$ is significantly suppressed compared to that of the lattice [7]; to reproduce the lattice result, one has to artificially

increase the value of the gauge coupling from the correct value $\alpha_s = 0.22$ to $\alpha_s = 0.29$ [29].

It would seem, therefore, that the main reason for the observed discrepancy ought to be traced back to the way in which the fully dressed ghost-gluon vertex, Γ_ν , appearing in the ghost SDE, is approximated. Even though preliminary lattice studies indicate that the deviations of Γ_ν from its tree-level value are relatively moderate [30–34], the highly non-linear nature of the ghost SDE may lead to considerable enhancements. In fact, a modest increase of the relevant vertex form factor in the region of momenta that provide the largest support to the ghost SDE may account for the bulk of the required effect.

The purpose of this article is to obtain a reliable “first-principle” approximation for this important missing ingredient. Specifically, we will determine the relevant vertex form factor from an approximate version of the SDE satisfied by the vertex Γ_ν itself, in the LG. To be sure, the vertex SDE has a complicated skeleton expansion, involving various unknown (or only partially known) quantities, such as multiparticle kernels. The basic approximations we employ at the level of the vertex SDE are: (i) we consider only the first two diagrams in this expansion; this corresponds to the “one-loop dressed” truncation [35], and (ii) inside these diagrams we replace full vertices by their tree-level values, but keep *fully dressed* ghost and gluon propagators, (iii) for the numerical analysis of the resulting integrals, we use as input for the full gluon propagators the lattice data of [11].

The tensorial decomposition of Γ_ν consists of two form factors [see Eq. (2.2)]; however, given that this vertex will be inserted in the ghost SDE, written in the LG, only the co-factor $A(-k, -p, r)$ of the ghost momentum p_ν survives. In the present study we determine $A(-k, -p, r)$ for two particular kinematic configurations, soft gluon ($k \rightarrow 0$) and soft ghost ($p \rightarrow 0$), thus converting it, in both cases, to a function of a single momentum only, $A(0, -p, p)$ and $A(-k, 0, k)$, respectively. In fact, as we will explain in detail in Sec. III, the case where $p \rightarrow 0$ is equivalent to the standard Taylor limit [36, 37].

Our main results may be summarized as follows.

(i) In the soft gluon limit, the result obtained for $A(0, -p, p)$ displays a moderate peak around 1 GeV, corresponding to a 20% increase with respect to the tree-level value; this result compares rather well with the existing lattice data [32, 33]. Of course, this particular kinematic configuration is not relevant for the ghost SDE, but serves as a preliminary test of the overall faithfulness of the approximations employed.

(ii) The numerical solutions for the coupled system of integral equations determining

$F(p^2)$ and $A(-k, 0, k)$ gives rise to a ghost dressing function that is in excellent agreement with the lattice data [11]. The corresponding solution for $A(-k, 0, k)$ is characterized by a rather pronounced maximum, centered again around 1 GeV, reaching a value of about 1.5. In this analysis we use $\alpha_s = 0.22$, which corresponds to the momentum-subtraction (MOM) value for the point $\mu = 4.3$ GeV [38], used to renormalize the gluon propagator obtained from the lattice.

The article is organized as follows. In Sec. II we introduce the necessary notation, and set up the SDE for the ghost dressing function, paying particular attention to the way that the fully dressed ghost-gluon vertex enters in it. In Sec. III we carry out the analysis at the level of the SDE of the ghost-gluon vertex, and derive the corresponding closed expressions in the two kinematic limits of interest. In Sec. IV we present the numerical treatment of the equations derived in the previous sections. In particular, we first compute the case of the soft gluon, and then we proceed to the solution of the coupled system. Finally, our conclusions and discussion are presented in Sec. V.

II. GHOST DRESSING FUNCTION AND THE GHOST-GLUON VERTEX

In this section we introduce the SDE for the ghost propagator in the LG, and discuss some of its basic properties and features. Of particular interest is the dependence of this equation on the surviving component of the ghost-gluon vertex, and the numerical implications of approximating it by its tree-level value.

Our starting point is the full ghost-gluon vertex, shown in Fig. 1, and denoted by

$$\Gamma_\nu^{nbc}(-k, -p, r) = g f^{nbc} \Gamma_\nu(-k, -p, r), \quad r = k + p, \quad (2.1)$$

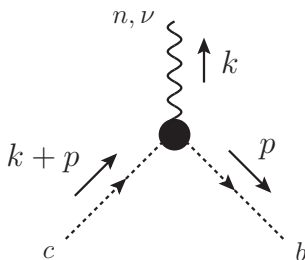


FIG. 1: The fully dressed ghost-gluon vertex.

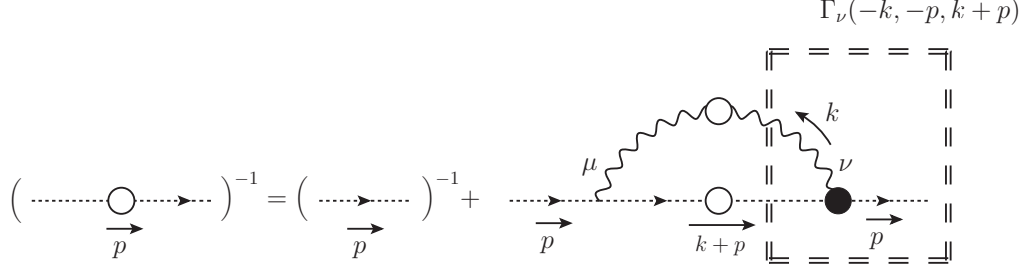


FIG. 2: The SDE for the ghost propagator given by Eq. (2.7). The white blobs represent the fully dressed gluon and ghost propagators, while the black blob denotes the dressed ghost-gluon vertex.

with k representing the momentum of the gluon and p of the anti-ghost. The most general tensorial structure of this vertex is given by

$$\Gamma_\nu(-k, -p, r) = A(-k, -p, r) p_\nu + B(-k, -p, r) k_\nu; \quad (2.2)$$

at tree-level, the two form factors assume the values $A^{[0]}(-k, -p, r) = 1$ and $B^{[0]}(-k, -p, r) = 0$, giving rise to the bare ghost-gluon vertex $\Gamma_\nu^{[0]} = p_\nu$.

The form factors A and B may be formally projected out by contracting Γ_ν with the vectors

$$\varepsilon_\nu^A(k, p) = \frac{k^2 p_\nu - (k \cdot p) k_\nu}{k^2 p^2 - (k \cdot p)^2}, \quad \varepsilon_\nu^B(k, p) = \frac{p^2 k_\nu - (k \cdot p) p_\nu}{k^2 p^2 - (k \cdot p)^2}, \quad (2.3)$$

namely

$$A(-k, -p, r) = \varepsilon_\nu^A(k, p) \Gamma^\nu(-k, -p, r), \quad B(-k, -p, r) = \varepsilon_\nu^B(k, p) \Gamma^\nu(-k, -p, r). \quad (2.4)$$

Of particular importance for the analysis that follows is the so-called “Taylor limit” of the ghost-gluon vertex, corresponding to the case of vanishing ghost momentum, $r = 0$, $p = -k$. In this special kinematic configuration, the $\Gamma_\nu(-k, -p, r)$ of Eq. (2.2) becomes

$$\Gamma_\nu(-k, k, 0) = -[A(-k, k, 0) - B(-k, k, 0)]k_\nu. \quad (2.5)$$

Closely related to this limit is the well-known Taylor theorem, which states that, to all orders in perturbation theory,

$$A(-k, k, 0) - B(-k, k, 0) = 1; \quad (2.6)$$

as a result, the fully-dressed vertex assumes the tree-level value corresponding to this particular kinematic configuration, *i.e.*, $\Gamma_\nu(-k, k, 0) = -k_\nu$.

After these introductory comments, let us turn to the SDE for the ghost propagator, and examine in some detail how the ghost-gluon vertex affects its structure. The relevant SDE is diagrammatically represented in the Fig. 2. Using the momenta flow and Lorentz indices as indicated in Fig. 2, the ghost SDE can be written as

$$iD^{-1}(p^2) = ip^2 - g^2 C_A \int_k \Gamma_\mu^{[0]}(k, -k - p, p) \Delta^{\mu\nu}(k) \Gamma_\nu(-k, -p, k + p) D(k + p), \quad (2.7)$$

where C_A denotes the Casimir eigenvalue of the adjoint representation (N for $SU(N)$), $d = 4 - \epsilon$ is the space-time dimension, and we have introduced the integral measure

$$\int_k \equiv \frac{\mu^\epsilon}{(2\pi)^d} \int d^d k, \quad (2.8)$$

with μ the 't Hooft mass. In the LG, the gluon propagator $\Delta_{\mu\nu}(q)$ has the transverse form

$$\Delta_{\mu\nu}(q) = -i P_{\mu\nu}(q) \Delta(q^2), \quad (2.9)$$

with

$$P_{\mu\nu}(q) = g_{\mu\nu} - \frac{q_\mu q_\nu}{q^2}, \quad (2.10)$$

the usual projection operator.

Clearly, due to the full transversality of $\Delta_{\mu\nu}(k)$, any reference to the form factor B disappears from the ghost SDE of Eq. (2.7). Specifically, substituting Eq. (2.2) into Eq. (2.7) we obtain

$$F^{-1}(p^2) = 1 + ig^2 C_A \int_k \left[1 - \frac{(k \cdot p)^2}{k^2 p^2} \right] A(-k, -p, k + p) \Delta(k) D(k + p), \quad (2.11)$$

where we have introduced the ghost dressing function, $F(q^2)$, defined as

$$D(q^2) = \frac{F(q^2)}{q^2}. \quad (2.12)$$

The renormalization of Eq. (2.11) proceeds through the replacements

$$\begin{aligned} \Delta_R(q^2) &= Z_A^{-1} \Delta(q^2), \\ F_R(q^2) &= Z_c^{-1} F(q^2), \\ \Gamma_R^\nu(q, p, r) &= Z_1 \Gamma^\nu(q, p, r), \\ g_R &= Z_g^{-1} g = Z_1^{-1} Z_A^{1/2} Z_c g, \end{aligned} \quad (2.13)$$

where Z_A , Z_c , Z_1 , and Z_g are the corresponding renormalization constants; the dependence of the above quantities on the renormalization point μ is suppressed. In the MOM scheme,

usually employed in the SDE analysis, the renormalization conditions imposed are that at μ the corresponding Green's functions assume their tree-level values, e.g., $\Delta_R^{-1}(q^2 = \mu^2) = \mu^2$, and $F_R(q^2 = \mu^2) = 1$ [37]. Note also that, in the LG, the form factor A is ultraviolet finite at one-loop, and therefore, no infinite renormalization constant needs to be introduced at that order for Γ^ν . In fact, one usually invokes Taylor's theorem [see Eq. (2.6)], in order to finally set $Z_1 = 1$ to all orders (see discussion in Sec. III).

Then, the SDE becomes

$$F^{-1}(p^2) = Z_c + ig^2 C_A \int_k \left[1 - \frac{(k \cdot p)^2}{k^2 p^2} \right] A(-k, -p, k+p) \Delta(k) D(k+p), \quad (2.14)$$

where we have suppressed the subscript “R” to avoid notation clutter. The actual closed expression of Z_c is obtained from Eq. (2.14) itself, by imposing the aforementioned MOM renormalization condition on $F^{-1}(p^2)$.

Evidently, the explicit dependence of Eq. (2.14) on $A(-k, -p, k+p)$ requires the use of the corresponding vertex SDE, thus converting the problem of determining $F(p^2)$ into a coupled SDE system. The usual way to circumvent this technical complication has been to simply approximate $A(-k, -p, k+p)$ by its tree-level value, setting into Eq. (2.14) $A(-k, -p, k+p) = 1$.

Then, after proper renormalization along the lines discussed above, and passing to the Euclidean space following the standard rules, one solves Eq. (2.14) numerically, using the lattice data of [11] as input for the gluon propagator. Note that this latter propagator is renormalized within the MOM scheme, by imposing the standard condition $\Delta^{-1}(\mu^2) = \mu^2$ at $\mu = 4.3$ GeV, namely the deepest available point in this set of lattice data; then, the corresponding value for $\alpha_s = g^2/4\pi$ that one should use is $\alpha_s(4.3\text{GeV}) = 0.22$. However, for this particular value of α_s , the solution obtained from Eq. (2.14) lies considerably below the lattice data for $F(p^2)$, as can be clearly seen from the (blue) dotted curve of Fig. 3. In order to obtain a close coincidence with the lattice, one must increase the value of $\alpha_s(4.3\text{GeV})$ to 0.29, thus obtaining the (red) continuous curve in Fig. 3.

It is, of course, natural to attribute the observed discrepancy to the aforementioned simple approximation employed for the ghost-gluon vertex. Therefore, to ameliorate the situation, we will determine this form factor from its corresponding SDE, in a certain kinematic limit that is relevant for the situation at hand. Specifically, given that $A(-k, -p, k+p)$ is a function of three variables, p^2 , k^2 , and the angle between the two (appearing in the inner

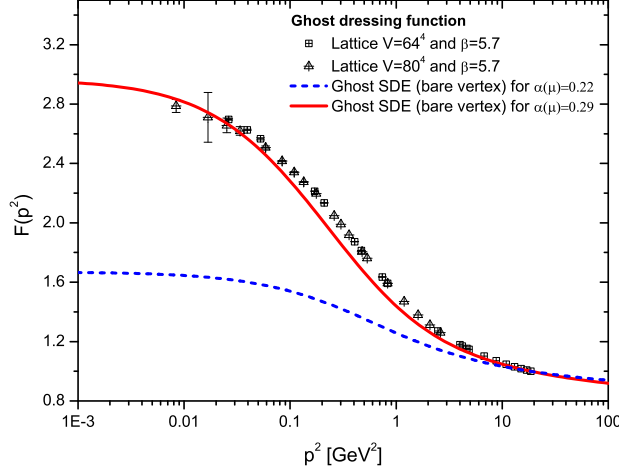


FIG. 3: Comparison of the ghost dressing function, $F(p^2)$, obtained as solution of the ghost SDE when the ghost-gluon vertex is approximate by its bare value, with the lattice data of Ref. [11]. The (red) continuous curve represents the case when $\alpha_s(4.3\text{GeV}) = 0.29$ whereas the (blue) dotted curve is obtained when $\alpha_s(4.3\text{GeV}) = 0.22$.

product $p \cdot k$), a full SDE treatment is rather cumbersome, and lies beyond our present technical powers. Instead, we will consider the behavior of $A(-k, -p, k + p)$ for vanishing p ; to that end, we start out with the Taylor expansion of $A(-k, -p, k + p)$ around $p = 0$, and we only keep the first term, $A(-k, 0, k)$, thus converting A into a function of a single variable.

We emphasize that the limit $p \rightarrow 0$ is taken only inside the argument of the form factor A , but not in the rest of the terms appearing in the SDE of Eq. (2.14). Specifically, following the procedure explained in detail in the next section, one isolates from the ghost-gluon SDE the contribution proportional to p_ν , taking the limit $p \rightarrow 0$ in the accompanying scalar co-factor, thus arriving at a form $\Gamma_\nu(-k, -p, k + p) = p_\nu A(-k, 0, k)$. Equivalently, in terms of the projectors introduced in Eqs. (2.3) and (2.4), one has

$$A(-k, 0, k) = \lim_{p \rightarrow 0} \{ \varepsilon_\nu^A(k, p) \Gamma^\nu(-k, -p, k + p) \}. \quad (2.15)$$

Thus, the approximate version of the SDE in Eq. (2.14) reads

$$F^{-1}(p^2) = Z_c + ig^2 C_A \int_k \left[1 - \frac{(k \cdot p)^2}{k^2 p^2} \right] A(-k, 0, k) \Delta(k) D(k + p). \quad (2.16)$$

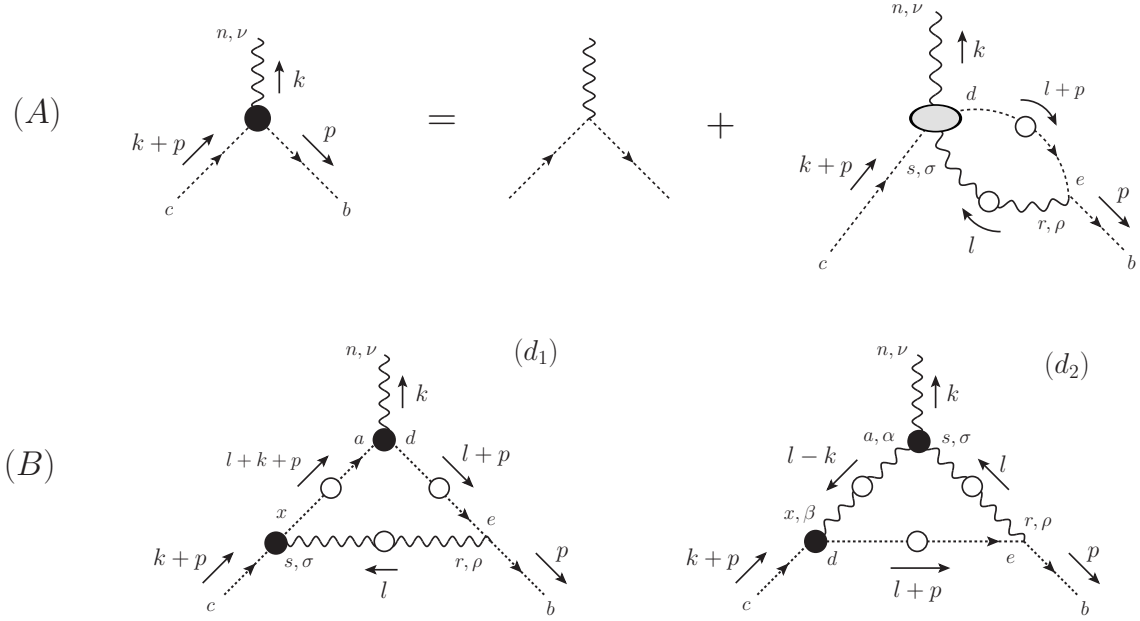


FIG. 4: (A) The complete SDE of the ghost-gluon vertex. Notice that we have set up it with respect to the anti-ghost leg. (B) Diagrams included in the skeleton expansion of the ghost-gluon kernel that we will consider in our analysis.

III. THE GHOST-GLUON VERTEX

In this section we derive in detail the nonperturbative expression for the form factor A , in two special kinematic configurations: (i) the *soft gluon limit*, in which the momentum carried by the gluon leg is zero ($k = 0$), and (ii) the *soft ghost limit*, where the momentum of the anti-ghost leg vanishes ($p = 0$).

A. General considerations

The starting point of our analysis is the SDE satisfied by the ghost-gluon vertex, whose diagrammatic representation is shown in panel (A) of Fig. 4. One observes that the relevant quantity, which controls the dynamics of this SDE, is the four-point ghost-gluon kernel.

For the ensuing analysis we will carry out the following main simplifications:

(i) The ghost-gluon kernel will be replaced by its “one-loop dressed” approximation; specifically, in the corresponding skeleton expansion we will only include the diagrams appearing in panel (B) of Fig. 4. Thus, the approximate version of the SDE that we employ

may be cast in the form

$$\Gamma_\nu(-k, -p, k+p) = p_\nu - \frac{i}{2}g^2 C_A [(d_1)_\nu - (d_2)_\nu], \quad (3.1)$$

where the diagrams (d_i) are given by

$$\begin{aligned} (d_1)_\nu &= \int_l \Gamma_\rho^{[0]} \Delta^{\rho\sigma}(l) \Gamma_\sigma D(l+k+p) \Gamma_\nu D(l+p), \\ (d_2)_\nu &= \int_l \Gamma_\rho^{[0]} \Delta^{\rho\sigma}(l) \Gamma_{\nu\sigma\alpha} \Delta^{\alpha\beta}(l-k) \Gamma_\beta D(l+p). \end{aligned} \quad (3.2)$$

For notational simplicity, we have suppressed the arguments of the momenta in all vertices; the latter may be easily recovered from the figures and the conventions established in Sec. II. Note also that, in the LG that we use, the gluon propagators appearing in the above expressions assume the completely transverse form of Eq. (2.9).

(ii) The (multiplicative) renormalization of Eq. (3.1) proceeds in the standard way. Specifically, in addition to the renormalization constants and relations given in Eq. (2.13), one must introduce the vertex renormalization for the three-gluon vertex, to be denoted by Z_3 , namely $\Gamma_R^{\nu\sigma\alpha} = Z_3 \Gamma^{\nu\sigma\alpha}$, together with the corresponding relation for the coupling renormalization, namely $g_R = Z_3^{-1} Z_A^{3/2} g$. From this relation, and the last of Eq. (2.13), one has that $Z_3^{-1} Z_A = Z_1^{-1} Z_c$. Then, it is straightforward to show that the contributions of $g^2(d_1)_\nu$ and $g^2(d_2)_\nu$ maintain the same form after renormalization; in fact, this property may be easily established by grouping the integrands in terms of the standard renormalization-group invariant quantities formed by $(g\Gamma_\mu \Delta^{1/2} D)$ and $(g\Gamma^{\nu\sigma\alpha} \Delta^{3/2})$ [39]. Thus, the renormalized version of Eq. (3.1) reads

$$\Gamma_R^\nu(-k, -p, k+p) = Z_1 \left\{ p_\nu - \frac{i}{2}g_R^2 C_A [(d_1)_R^\nu - (d_2)_R^\nu] \right\}, \quad (3.3)$$

where the Z_1 comes from the renormalization of the $\Gamma^\nu(-k, -p, k+p)$ on the lhs.

In what follows we will set $Z_1 = 1$. In the case of the soft ghost configuration, $p = 0$, (which, as we will see, is equivalent to the Taylor kinematics), this choice is imposed by Taylor's theorem, see Eq. (2.6). On the other hand, in the case of the soft gluon configuration, $k = 0$, this choice constitutes an approximation, in the sense that it is motivated by the one-loop finiteness of the (LG) Γ^ν , but is not enforced by an analogous all-order relation.

(iii) In the two aforementioned diagrams, (d_1) and (d_2) , we will keep fully dressed propagators, but will replace the fully dressed three-gluon vertex appearing in graph (d_2) by the

corresponding tree-level expression, namely

$$\Gamma_{\alpha\mu\nu}(q, r, p) \rightarrow \Gamma_{\alpha\mu\nu}^{[0]}(q, r, p) = (r - p)_\alpha g_{\mu\nu} + (p - q)_\mu g_{\nu\alpha} + (q - r)_\nu g_{\alpha\mu}. \quad (3.4)$$

Furthermore, as will be explained in the corresponding subsections, additional approximations will be imposed on the fully dressed ghost-gluon vertices, depending on the specific details of each kinematic case considered.

B. Soft gluon configuration

We begin with the analysis of the soft gluon configuration, $k = 0$. Evidently, in this case the ghost-gluon vertex becomes a function of only one momentum, p , and may be described in terms of a single form factor, namely,

$$\Gamma_\nu(0, -p, p) = A(p)p_\nu; \quad A(p) \equiv A(0, -p, p). \quad (3.5)$$

Therefore, setting $k = 0$ in Eq. (3.1), one is able to isolate the form factor A by means of the projection

$$A(p) = 1 - \frac{i}{2}g^2 C_A [(d_1) - (d_2)]; \quad (d_i) \equiv \frac{p^\nu}{p^2} (d_i)_\nu, \quad i = 1, 2, \quad (3.6)$$

where the diagrams (d_i) are obtained from those of Eq. (3.2) in the limit $k \rightarrow 0$.

The particular kinematic configuration considered here allows one to derive a linear integral equation for the unknown quantity $A(p)$. This becomes possible because, in the limit $k = 0$, the vertex Γ_ν entering in graph (d_1) becomes $\Gamma_\nu(0, -l - p, l + p)$. Thus, the integral (d_1) contains $A(0, -l - p, l + p)$, giving rise to an integral equation for $A(0, -p, p)$. Unfortunately, this favorable set of circumstances does not apply to the remaining ghost-gluon vertices, namely, Γ_σ and Γ_β in graphs (d_1) and (d_2) , respectively; their arguments depend on all possible kinematic variables, and the inclusion of the full A would give rise to a (non-linear) integral equation, too complicated to solve. We therefore approximate all remaining ghost-gluon vertices by their tree-level expressions.

After these comments, and use of the notation introduced in Eq. (3.6), the diagram (d_1) reads

$$(d_1) = \int_l \frac{(l \cdot p)}{(l + p)^2 p^2} [(l \cdot p)^2 - l^2 p^2] D^2(l) \Delta(l + p) A(l). \quad (3.7)$$

To evaluate the contribution of diagram (d_2) notice that, with the gluon propagators in the LG, and the bare three-gluon vertex of Eq. (3.4), we have that

$$P^{\rho\sigma}(l)P^{\alpha\beta}(l)\Gamma_{\nu\sigma\alpha}^{[0]}(0,l,-l) = 2l_\nu P^{\rho\beta}(l). \quad (3.8)$$

Applying this result we get

$$(d_2) = 2 \int_l \frac{(l \cdot p)}{l^2 p^2} [l^2 p^2 - (l \cdot p)^2] \Delta^2(l) D(l+p). \quad (3.9)$$

The final answer is obtained by substituting Eq. (3.7) and Eq. (3.9) into Eq. (3.6); it will be written directly in Euclidean space, using the standard transformation rules,

$$-q^2 = q_E^2; \quad \Delta_E(q_E^2) = -\Delta(-q_E^2); \quad D_E(q_E^2) = -D(-q_E^2); \quad \int_k = i \int_{k_E}, \quad (3.10)$$

and setting

$$l^2 = t; \quad p^2 = x; \quad (l+p)^2 = z; \quad (l \cdot p) = \sqrt{xt} \cos \theta; \\ \int_{l_E} = \int \frac{d^4 l}{(2\pi)^4} = \frac{1}{(2\pi)^3} \int_0^\infty dt t \int_0^\pi d\theta \sin^2 \theta. \quad (3.11)$$

Specifically (we suppress the subscript “E”),

$$A(x) = 1 - \frac{\alpha_s C_A}{4\pi^2} \int_0^\infty dt \sqrt{xt} F^2(t) A(t) \int_0^\pi d\theta \sin^4 \theta \cos \theta \left[\frac{\Delta(z)}{z} \right] \\ - \frac{\alpha_s C_A}{2\pi^2} \int_0^\infty dt \sqrt{xt} t \Delta^2(t) \int_0^\pi d\theta \sin^4 \theta \cos \theta \left[\frac{F(z)}{z} \right], \quad (3.12)$$

where we have used $g^2 = 4\pi\alpha_s$, and Eq. (2.12) in order to express the ghost propagators in terms of their dressing functions.

Notice that, in the limit $x = 0$, namely when the momentum of the ghost leg is also zero, we recover from Eq. (3.12) the tree-level value of the form factor, *i.e.*, $A(0) = 1$.

C. Soft ghost configuration (Taylor kinematics)

We next turn to the case that, according to the discussion presented in Sec. II, is expected to improve the treatment of the ghost SDE. Specifically, in this subsection we will derive an approximate version for A in the soft ghost configuration, to be denoted by

$$\lim_{p \rightarrow 0} A(-k, -p, k+p) = A(-k, 0, k) \equiv A(k). \quad (3.13)$$

However, before proceeding to this derivation, we will demonstrate that the form factor $A(-k, 0, k)$ obtained in the soft ghost configuration is none other than the form factor $A(-k, k, 0)$, appearing in the constraint imposed by Taylor's theorem, given by Eq. (2.6). To prove that, let us rewrite the SDE of the ghost propagator, Eq. (2.7), dressing this time the left ghost-gluon vertex instead of the right, *i.e.*,

$$iD^{-1}(p^2) = ip^2 - g^2 C_A \int_k \Gamma_\mu(k, -k - p, p) \Delta^{\mu\nu}(k) \Gamma_\nu^{[0]}(-k, -p, k + p) D(k + p), \quad (3.14)$$

where we have maintained the same momenta flow and Lorentz indices as in Fig. 2. Therefore, using Eq. (2.2) for the Γ_μ in Eq. (3.14), we get (in the LG)

$$F^{-1}(p^2) = 1 + ig^2 C_A \int_k \left[1 - \frac{(k \cdot p)^2}{k^2 p^2} \right] A(k, -k - p, p) \Delta(k) D(k + p). \quad (3.15)$$

Evidently Eqs. (2.11) and (3.15) must furnish an identical result for $F(p^2)$, since the answer cannot depend on which of the two vertices one chooses to dress. Thus, the form factor A is forced to satisfy the equality

$$A(-k, -p, k + p) = A(k, -k - p, p). \quad (3.16)$$

Given that, due to Lorentz invariance, the dependence on the momenta is quadratic, *i.e.*, $A(k^2, p^2, k^2 + p^2 + 2k \cdot p)$, we have immediately that

$$A(k, -k - p, p) = A(-k, k + p, -p). \quad (3.17)$$

So, combining Eqs. (3.16) and (3.17), we arrive at the relation

$$A(-k, -p, k + p) = A(-k, k + p, -p), \quad (3.18)$$

which states that, in the LG, the form factor A of the gluon-ghost vertex is invariant under the exchange of the momenta of the ghost and anti-ghost legs. Notice that this invariance is known to be a consequence of a global $SL(2, R)$ symmetry between the ghost and anti-ghost fields [2], which implies that the LG is a ghost-anti-ghost symmetric gauge fixing choice. Finally, setting $p = 0$ in Eq. (3.18), one obtains the announced result, that is, the A obtained in the soft ghost limit coincides with that of the Taylor kinematics.

As mentioned above, the fact that the kinematic situation considered here is equivalent to the Taylor limit, imposes, in a natural way, the value $Z_1 = 1$ for the renormalization constant appearing in Eq. (3.3).

Once the above connection has been established, we return to the derivation of the explicit expression for the form factor A in the soft ghost limit. To that end, we will consider again the diagrams shown in panel (B) of Fig. 4, with dressed gluon and ghost propagators, and tree-level values for *all* the interaction vertices. In this configuration, the expressions given in Eq. (3.2) reduce to

$$\begin{aligned}(d_1)_\nu &= p^\rho(k+p)^\sigma \int_l (l+p)_\nu D(l+p) D(l+k+p) \Delta(l) P_{\rho\sigma}(l), \\(d_2)_\nu &= p^\rho(k+p)^\beta \int_l D(l+p) \Delta(l) \Delta(l-k) P_\rho^\sigma(l) P_\beta^\alpha(l-k) \Gamma_{\nu\sigma\alpha}^{[0]},\end{aligned}\quad (3.19)$$

We next outline the general procedure for isolating the $A(-k, 0, k)$ defined in Eq. (3.13). First, we observe that the most general Lorentz decomposition of the diagrams given in Eq. (3.19) is

$$\begin{aligned}(d_i)_\nu &= p^\rho(k+p)^\sigma [f_1 g_{\nu\rho} k_\sigma + f_2 g_{\nu\sigma} k_\rho + f_3 g_{\rho\sigma} k_\nu + f_4 g_{\nu\rho} p_\sigma + f_5 g_{\nu\sigma} p_\rho + f_6 g_{\rho\sigma} p_\nu \\&+ f_7 p_\nu p_\rho p_\sigma + f_8 p_\nu p_\rho k_\sigma + f_9 p_\nu k_\rho p_\sigma + f_{10} p_\nu k_\rho k_\sigma + f_{11} k_\nu k_\rho k_\sigma + f_{12} k_\nu k_\rho p_\sigma \\&+ f_{13} k_\nu p_\rho k_\sigma + f_{14} k_\nu p_\rho p_\sigma],\end{aligned}\quad (3.20)$$

where the corresponding form factors $f_i \equiv f_i(k, p)$ are assumed to be finite in the infrared limit $p \rightarrow 0$.

A detailed look at this expansion reveals that only the tensorial structure $g_{\nu\rho} k_\sigma$, accompanying the form factor f_1 , can saturate the prefactor $p^\rho(k+p)^\sigma$ and survive when the limit $p \rightarrow 0$ is taken. Specifically, we may rewrite Eq. (3.20) as follows

$$\begin{aligned}(d_i)_\nu &= p^\rho k^\sigma f_1(k, p) g_{\nu\rho} k_\sigma + \mathcal{O}(p)(k+p)_\nu \\&= k^2 f_1(k, p) p_\nu + \mathcal{O}(p)(k+p)_\nu,\end{aligned}\quad (3.21)$$

where the symbol $\mathcal{O}(p)(k+p)_\nu$ is used to indicate terms that saturate with p_ν or k_ν , but whose form factors are of order $\mathcal{O}(p)$ or higher, and will not contribute in the soft ghost configuration. Furthermore, one can perform the Taylor expansion of $f_1(k, p)$ around $p = 0$, namely,

$$f_1(k, p) = f_1(k, 0) + 2(k \cdot p) f_1'(k) + \mathcal{O}(p^2); \quad f_1'(k) \equiv \left. \frac{\partial}{\partial p^2} f_1(k, p) \right|_{p=0}. \quad (3.22)$$

Thus, only the zero order term of this expansion is relevant for our kinematic configuration, and we obtain finally from Eq. (3.21) the following result

$$(d_i)_\nu = k^2 f_1(k, 0) p_\nu + \mathcal{O}(p)(k+p)_\nu, \quad (3.23)$$

where the quantity $k^2 f_1(k, 0)$ should be identified as the contribution of the corresponding diagram to $A(k)$, while terms containing the derivatives of f_1 are naturally reassigned to $\mathcal{O}(p)(k+p)_\nu$.

After these observations, it is relatively easy to establish that this generic procedure can be systematically implemented by performing the following steps: (i) Set $p = 0$ from the beginning *inside* the integrals of Eq. (3.19). (ii) Discard all the terms that give rise to structures of the type $\mathcal{O}(p)(k+p)_\nu$. (iii) Determine the contribution of the diagram that saturates the index of the momentum p^ρ with the metric tensor $g_{\nu\rho}$.

To illustrate in some detail the above procedure, let us focus our attention on the contribution of diagram (d_1) , appearing in the first line of Eq. (3.19). Applying step (i), we obtain

$$(d_1)_\nu = p^\rho (k+p)^\sigma \left\{ \int_l l_\nu D(l) D(l+k) \Delta(l) P_{\rho\sigma}(l) + p_\nu \int_l D(l) D(l+k) \Delta(l) P_{\rho\sigma}(l) \right\}. \quad (3.24)$$

Now, using criterion (ii), it is easy to recognize that the part of Eq. (3.24) to be retained is given by

$$(d_1)_\nu = -p^\rho I_{\nu\rho}(k), \quad (3.25)$$

where we have defined the integral

$$I_{\nu\rho}(k) = \int_l \frac{(l \cdot k)}{l^2} D(l) D(l+k) \Delta(l) l_\nu l_\rho, \quad (3.26)$$

which may be further decomposed as

$$I_{\nu\rho}(k) = I_1(k^2) g_{\nu\rho} + I_2(k^2) k_\nu k_\rho, \quad (3.27)$$

with

$$I_1(k^2) = \frac{1}{d-1} P^{\nu\rho}(k) I_{\nu\rho}(k); \quad I_2(k^2) = \frac{1}{k^4(d-1)} (dk^\nu k^\rho - k^2 g^{\nu\rho}) I_{\nu\rho}(k). \quad (3.28)$$

Thus, using Eqs. (3.27) and (3.28), we obtain from Eq. (3.25) the following result

$$(d_1)_\nu = -\frac{1}{d-1} p_\nu \int_l \frac{(l \cdot k)}{l^2 k^2} [l^2 k^2 - (l \cdot k)^2] D(l) D(l+k) \Delta(l), \quad (3.29)$$

where, according to (iii), we have only written explicitly the contribution that saturates the momentum p^ρ with the metric tensor $g_{\nu\rho}$.

Consider finally the contribution of diagram (d_2) . After the shift $l \mapsto -l$, and setting $p = 0$ inside the integral, it becomes

$$(d_2)_\nu = p^\rho (k+p)^\beta \int_l D(l) \Delta(l) \Delta(l+k) P_\rho^\sigma(l) P_\beta^\alpha(l+k) \Gamma_{\nu\sigma\alpha}^{[0]}. \quad (3.30)$$

It is then elementary to show that

$$\begin{aligned} p^\rho (k+p)^\beta P_\rho^\sigma(l) P_\beta^\alpha(l+k) \Gamma_{\nu\sigma\alpha}^{[0]} &= 2p^\rho \frac{l_\nu l_\rho}{l^2(l+k)^2} [l^2 k^2 - (l \cdot k)^2 + (l+k)^2 (l \cdot k)] \\ &\quad + 2p_\nu \frac{[(l \cdot k)^2 - l^2 k^2]}{(l+k)^2} + \mathcal{O}(p)(k+p)_\nu, \end{aligned} \quad (3.31)$$

and, therefore, the part of diagram (d_2) to be saved is

$$(d_2)_\nu = 2p_\nu \int_l \frac{[(l \cdot k)^2 - l^2 k^2]}{(l+k)^2} D(l) \Delta(l) \Delta(l+k) + 2p^\rho Q_{\nu\rho}(k), \quad (3.32)$$

where we have defined the integral

$$Q_{\nu\rho}(k) = \int_l \frac{l_\nu l_\rho}{l^2(l+k)^2} [l^2 k^2 - (l \cdot k)^2 + (l+k)^2 (l \cdot k)] D(l) \Delta(l) \Delta(l+k). \quad (3.33)$$

One observes at this point that the first term in Eq. (3.32) is already saturated by p_ν and may be assigned to the form factor $A(k)$ without further considerations. On the other hand, decomposing the integral Eq. (3.33) in the second term as

$$Q_{\nu\rho}(k) = Q_1(k^2) g_{\nu\rho} + Q_2(k^2) k_\nu k_\rho, \quad (3.34)$$

with

$$Q_1(k^2) = \frac{1}{d-1} P^{\nu\rho}(k) Q_{\nu\rho}(k); \quad Q_2(k^2) = \frac{1}{k^4(d-1)} (dk^\nu k^\rho - k^2 g^{\nu\rho}) Q_{\nu\rho}(k). \quad (3.35)$$

we obtain from Eq. (3.32) the result

$$(d_2)_\nu = \frac{2}{d-1} p_\nu \int_l \frac{[l^2 k^2 - (l \cdot k)^2]}{l^2 k^2 (l+k)^2} [(l+k)^2 (l \cdot k) - (l \cdot k)^2 - (d-2) l^2 k^2] D(l) \Delta(l) \Delta(l+k), \quad (3.36)$$

where, as before, we have omitted terms of the type $\mathcal{O}(p)(k+p)_\nu$.

Once Eqs. (3.29) and (3.36) have been derived, we will use Eq. (3.6) for projecting out the form factor $A(k)$, as well as Eqs. (3.10) and (3.11), in order to pass to Euclidean space, and subsequently cast the answer in spherical coordinates. Thus, we arrive at the final result

$$\begin{aligned} A(y) &= 1 - \frac{\alpha_s C_A}{12\pi^2} \int_0^\infty dt \sqrt{yt} F(t) \Delta(t) \int_0^\pi d\theta' \sin^4 \theta' \cos \theta' \left[\frac{F(u)}{u} \right] \\ &\quad + \frac{\alpha_s C_A}{6\pi^2} \int_0^\infty dt F(t) \Delta(t) \int_0^\pi d\theta' \sin^4 \theta' \left[\frac{\Delta(u)}{u} \right] [yt(1 + \sin^2 \theta') - (y+t) \sqrt{yt} \cos \theta']. \end{aligned} \quad (3.37)$$

Notice that, in this case, $y = k^2$, $u = (l+k)^2$, and θ' is the angle between k and l .

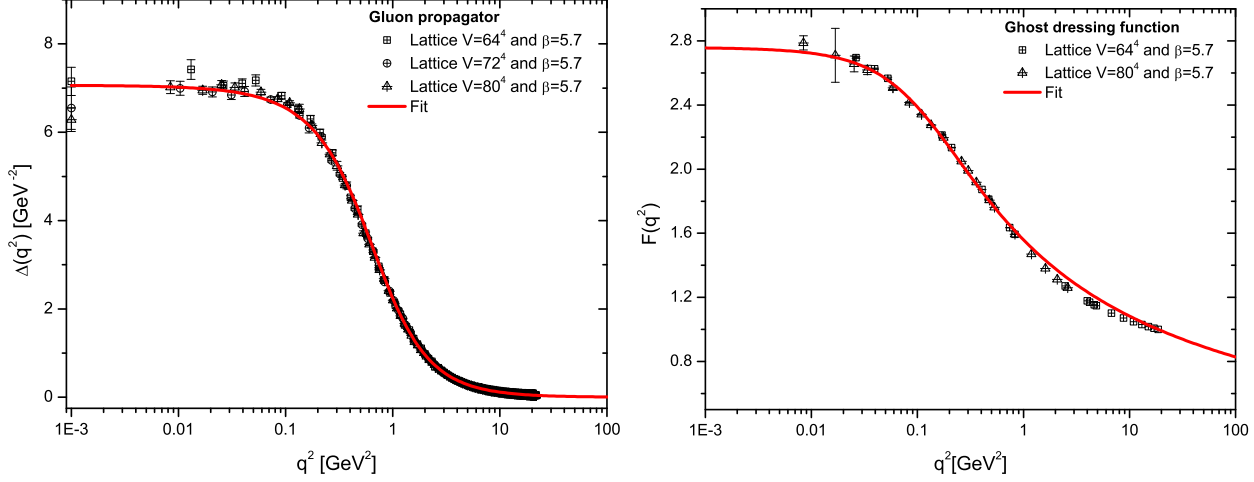


FIG. 5: Lattice results for the gluon propagator, $\Delta(q)$, (left panel) and ghost dressing, $F(q)$, (right panel) obtained in Ref. [11] and renormalized at $\mu = 4.3$ GeV. The (red) continuous curves represent the corresponding fits for the lattice data.

IV. NUMERICAL RESULTS

In this section we will carry out a detailed numerical analysis of the equations obtained in the previous sections. Specifically, in the first subsection we determine $A(0, -p, p)$ by solving the integral equation Eq. (3.12), using the lattice data of [11] as input for the gluon propagator $\Delta(q)$ and the ghost dressing function $F(q)$ appearing in it. The solution obtained is then compared with the lattice data of [32, 33]. In the second subsection, we solve numerically the coupled system formed by the integral equations of the ghost dressing function (2.16) and of the ghost-gluon vertex in the soft ghost configuration, given by (3.37). The unique external ingredient used when solving this system are the lattice data for the gluon propagator $\Delta(q)$. The solution obtained for $F(q)$ compares very favorably with the lattice data of [11].

A. Solution for the soft gluon configuration

The integral equation (3.12) is solved through an iterative process, using as input for the gluon propagator and the ghost dressing function the data obtained from the $SU(3)$ quenched simulations of [11], shown in Fig. 5. Note that the lattice data shown have been renormalized at $\mu = 4.3$ GeV, within the MOM scheme. The value of α_s that corresponds

to this value of μ may be obtained from the higher-order calculation presented in [38]; specifically, we have that $\alpha_s(\mu) = 0.22$.

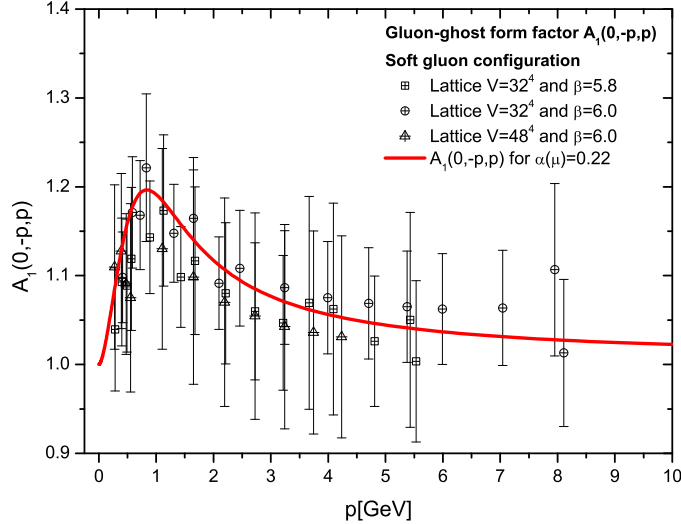


FIG. 6: Numerical result for $A(0, -p, p)$, obtained from Eq. (3.12) when $\alpha_s(\mu) = 0.22$.

The (red) continuous line in Fig. 6 represents the corresponding solution for $A(0, -p, p)$. We clearly see that $A(0, -p, p)$ develops a sizable peak around the momentum region of 830 MeV. In addition, as had been anticipated in the subsection III B, we confirm numerically that A indeed assumes its tree level value when $p \rightarrow 0$, *i.e.*, $A = 1$. It is also interesting to notice that, in the ultraviolet limit, the form factor gradually approaches its tree level value.

In Fig. 6, we compare our numerical results with the corresponding lattice data obtained in Ref. [32, 33] for this particular kinematic configuration. Although, the error bars are rather sizable, we clearly see that our solution follows the general structure of the data. In particular, notice that both peaks occur in the same intermediate region of momenta. Evidently, $A(0, -p, p)$ receives a significant non-perturbative correction, deviating considerably from its tree level value.

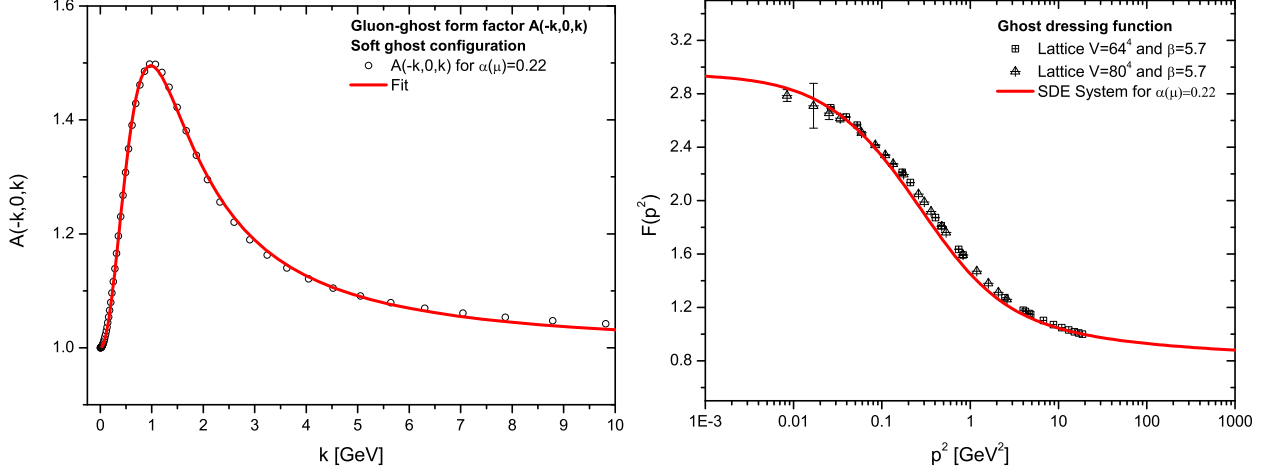


FIG. 7: *Left panel:* The form factor $A(-k, 0, k)$ (circles) and the fit given by Eq. (4.3) (red continuous line). *Right panel:* The numerical solution of $F(p)$ (red continuous line) compared with the lattice data of Ref. [11]. Note that the value of α_s used when solving the system is $\alpha_s(\mu) = 0.22$.

B. The coupled system: ghost SDE and ghost-gluon vertex.

In this subsection we present the central result of the present article, namely the modifications induced to the ghost dressing function by the inclusion of a non-trivial structure for the corresponding ghost-gluon vertex.

To that end, after passing to the Euclidean space and introducing spherical coordinates, using Eq. (3.10) and Eq. (3.11), we obtain from Eqs. (2.16) and (3.37) the expressions

$$F^{-1}(x) = 1 - \frac{\alpha_s C_A}{2\pi^2} \int_0^\infty dy y \Delta(y) A(y) \int_0^\pi d\theta \sin^4 \theta \left[\frac{F(z)}{z} - \frac{F(z')}{z'} \right]. \quad (4.1)$$

and

$$\begin{aligned} A(y) = & 1 - \frac{\alpha_s C_A}{12\pi^2} \int_0^\infty dt \sqrt{yt} F(t) \Delta(t) \int_0^\pi d\theta' \sin^4 \theta' \cos \theta' \left[\frac{F(u)}{u} \right] \\ & + \frac{\alpha_s C_A}{6\pi^2} \int_0^\infty dt F(t) \Delta(t) \int_0^\pi d\theta' \sin^4 \theta' \left[\frac{\Delta(u)}{u} \right] [yt(1 + \sin^2 \theta') - (y + t)\sqrt{yt} \cos \theta'], \end{aligned} \quad (4.2)$$

where now $z = (k + p)^2$, $z' = (k + \mu)^2$ and μ is the renormalization point introduced within the MOM scheme, *i.e.*, by requiring that $F^{-1}(\mu^2) = 1$.

We next solve the above system iteratively, using again the lattice data for $\Delta(q)$ and $\alpha_s(\mu) = 0.22$ as input. The results for $F(p)$ and $A(-k, 0, k)$ are shown in Fig. 7.

On the left panel of Fig. 7, the curve in circles represents the result for $A(-k, 0, k)$. Evidently, A develops a peak in the intermediate region of momenta, in a way similar to

the case discussed in the previous subsection. In this case the maximum of the peak occurs around 1 GeV, and once more, in the infrared and ultraviolet limits $A(-k, 0, k)$ assumes its tree-level value.

On the same panel we show a fit for $A(-k, 0, k)$, represented by the (red) continuous curve, whose functional form is given by

$$A(-k, 0, k) = 1 + \frac{ak^2}{[(k^2 + b)^2 + c] \ln(d + k^2/k_0^2)}, \quad (4.3)$$

with the following values for the fitting parameters $a = 0.68 \text{ GeV}^2$, $b = 0.72 \text{ GeV}^2$, $c = 0.29 \text{ GeV}^4$, $d = 9.62$ and $k_0^2 = 1 \text{ GeV}^2$.

On the right panel of Fig. 7, we compare our numerical result for $F(p)$ (red continuous curve) with the corresponding lattice data of Ref. [11], observing a rather notable agreement. We emphasize that, contrary to what happens when the bare vertex is used (see Fig. 3), the accuracy achieved here does not rely on the artificial enhancement of the value of the coupling; the latter, as mentioned above, was kept at its standard value predicted from general MOM considerations.

It is important to realize that, although A does not provide a sizable support for ghost SDE in the deep infrared, the contribution that it furnishes in the region of intermediate momenta is sufficient for increasing the saturation point from $F(0) = 1.67$ to $F(0) = 2.95$ (Figs. 3 and 7, respectively). This observation suggests that the ghost SDE is particularly sensitive to the values of its ingredients at momenta around two to three times the QCD mass scale.

V. CONCLUSIONS

In the present work we have considered the “one-loop dressed” approximation of the SDE that governs the evolution of the ghost-gluon vertex. In particular, we have focused on the dynamics of the form factor denoted by A , which is the one that survives in the SDE for ghost dressing function, in the LG. The vertex SDE has been evaluated for two special kinematic configurations, one of them corresponding to the well-known Taylor limit. When coupled to the SDE of the ghost, the contribution of this particular form factor accounts for the missing strength of the associated kernel, allowing one to reproduce the lattice results rather accurately, using the standard value of the gauge coupling constant.

The fact that, despite the truncation implemented on the vertex SDE, we finally obtained a rather good agreement with the lattice, hints to the possibility that the omitted terms are numerically subleading, at least in the case of the special kinematic configurations considered. It might be interesting to pursue this point further. Specifically, in the present analysis the terms proportional to the second form-factor, denoted by B , have been automatically discarded, precisely because they do not contribute to the ghost SDE. However, given that both form factors participate in the fundamental relation of Eq. (2.6), one might consider the possibility of keeping these terms throughout the calculation, and then checking explicitly to what extent Eq. (2.6) is satisfied in the present approximation.

Recently, the study of the effects that the dynamical quarks induce on some of the fundamental Green's functions of QCD has received particular attention, both from the point of view of unquenched lattice simulations [40], as well as by means of an SDE-based approach [41]. In particular, lattice simulations reveal that the inclusion of light active quarks results in a considerable suppression in the deep infrared and intermediate momentum region of the gluon propagator. This characteristic feature has been firmly established also within the SDE framework of [41]. On the other hand, the unquenched ghost dressing function simulated on the lattice suffers minimal changes from the inclusion of quarks [40]; this property has also been anticipated within the aforementioned SDE analysis [41], as a direct consequence of the fact that, in the case of F , the quark-loops enter as “higher-order” effects. In addition, it is well-known that the value of the MOM coupling, $\alpha(\mu)$, increases in the presence of quark loops.

It would be, therefore, interesting, to study the combination of these competing effects systematically, including the vertex equation for A , derived here. In particular, the non-linear nature of the corresponding integral equations converts this combined analysis into a rather challenging problem. Specifically, the changes induced to the integral equation for A , due to the aforementioned suppression of the gluon propagators entering in it, must be compensated, to a considerable level of accuracy, by the corresponding increase in the coupling constant, in order to finally obtain the rather minor change observed in F . We hope to be able to carry out such a study in the near future.

Acknowledgments

The research of J. P. is supported by the Spanish MEYC under grant FPA2011-23596. The work of A. C. A is supported by the National Council for Scientific and Technological Development - CNPq under the grant 306537/2012-5 and project 473260/2012-3, and by São Paulo Research Foundation - FAPESP through the project 2012/15643-1.

- [1] C. D. Roberts and A. G. Williams, Prog. Part. Nucl. Phys. **33**, 477 (1994).
- [2] R. Alkofer, L. von Smekal, Phys. Rept. **353**, 281 (2001).
- [3] C. S. Fischer, J. Phys. G **G32**, R253-R291 (2006).
- [4] D. Binosi and J. Papavassiliou, Phys. Rept. **479**, 1-152 (2009).
- [5] A. P. Szczepaniak and E. S. Swanson, Phys. Rev. D **65**, 025012 (2002).
- [6] A. P. Szczepaniak, Phys. Rev. D **69**, 074031 (2004).
- [7] A. C. Aguilar, D. Binosi and J. Papavassiliou, Phys. Rev. D **78**, 025010 (2008).
- [8] A. C. Aguilar and J. Papavassiliou, Phys. Rev. D **83**, 014013 (2011).
- [9] A. Cucchieri and T. Mendes, PoS **LAT2007**, 297 (2007); Phys. Rev. Lett. **100**, 241601 (2008); Phys. Rev. D **81**, 016005 (2010); PoS **LATTICE2010**, 280 (2010).
- [10] P. O. Bowman, U. M. Heller, D. B. Leinweber, M. B. Parappilly, A. Sternbeck, L. von Smekal, A. G. Williams and J. -b. Zhang, Phys. Rev. D **76**, 094505 (2007).
- [11] I. L. Bogolubsky, E. M. Ilgenfritz, M. Muller-Preussker and A. Sternbeck, PoS **LATTICE**, 290 (2007).
- [12] I. L. Bogolubsky, E. M. Ilgenfritz, M. Muller-Preussker and A. Sternbeck, Phys. Lett. B **676**, 69 (2009).
- [13] O. Oliveira, P. J. Silva, Phys. Rev. **D79**, 031501 (2009).
- [14] O. Oliveira and P. J. Silva, PoS **LAT2009**, 226 (2009).
- [15] M. R. Pennington and D. J. Wilson, Phys. Rev. D **84**, 119901 (2011).
- [16] A. Bashir, L. Chang, I. C. Cloet, B. El-Bennich, Y. -X. Liu, C. D. Roberts and P. C. Tandy, Commun. Theor. Phys. **58**, 79 (2012).
- [17] P. Boucaud, J-P. Leroy, A. L. Yaouanc, J. Micheli, O. Pene and J. Rodriguez-Quintero, JHEP **0806**, 012 (2008).

- [18] T. Kugo and I. Ojima, Prog. Theor. Phys. Suppl. **66**, 1 (1979).
- [19] T. Kugo, arXiv:hep-th/9511033.
- [20] P. Watson and R. Alkofer, Phys. Rev. Lett. **86** (2001) 5239.
- [21] K. -I. Kondo, Phys. Rev. D **84**, 061702 (2011).
- [22] D. Dudal, J. A. Gracey, S. P. Sorella, N. Vandersickel and H. Verschelde, Phys. Rev. D **78**, 065047 (2008).
- [23] J. M. Cornwall, Phys. Rev. D **26**, 1453 (1982).
- [24] A. C. Aguilar and J. Papavassiliou, JHEP **0612**, 012 (2006).
- [25] A. C. Aguilar and A. A. Natale, JHEP **0408**, 057 (2004).
- [26] D. Binosi and J. Papavassiliou, Phys. Rev. D **77**(R), 061702 (2008).
- [27] A. C. Aguilar, D. Binosi and J. Papavassiliou, JHEP **1201**, 050 (2012).
- [28] D. Dudal, O. Oliveira and J. Rodriguez-Quintero, Phys. Rev. D **86**, 105005 (2012).
- [29] A. C. Aguilar, D. Binosi and J. Papavassiliou, JHEP **1007**, 002 (2010).
- [30] A. Cucchieri, T. Mendes and A. Mihara, JHEP **0412**, 012 (2004).
- [31] E. M. Ilgenfritz, M. Muller-Preussker, A. Sternbeck and A. Schiller, arXiv:hep-lat/0601027.
- [32] E. -M. Ilgenfritz, M. Muller-Preussker, A. Sternbeck, A. Schiller and I. L. Bogolubsky, Braz. J. Phys. **37**, 193 (2007).
- [33] A. Sternbeck, hep-lat/0609016.
- [34] A. Cucchieri, A. Maas and T. Mendes, Phys. Rev. D **77**, 094510 (2008).
- [35] W. Schleifenbaum, A. Maas, J. Wambach and R. Alkofer, Phys. Rev. D **72**, 014017 (2005).
- [36] J. C. Taylor, Nucl. Phys. B **33**, 436 (1971).
- [37] W. J. Marciano and H. Pagels, Phys. Rept. **36**, 137 (1978).
- [38] P. Boucaud, F. De Soto, J. P. Leroy, A. Le Yaouanc, J. Micheli, O. Pene and J. Rodriguez-Quintero, Phys. Rev. D **79**, 014508 (2009).
- [39] A. C. Aguilar, D. Binosi, J. Papavassiliou and J. Rodriguez-Quintero, Phys. Rev. D **80**, 085018 (2009).
- [40] A. Ayala, A. Bashir, D. Binosi, M. Cristoforetti and J. Rodriguez-Quintero, Phys. Rev. D **86**, 074512 (2012).
- [41] A. C. Aguilar, D. Binosi and J. Papavassiliou, Phys. Rev. D **86**, 014032 (2012).